

THE POTENTIAL OF MULTI-PHASE ROTARY PRESSURE EXCHANGER INTEGRATION FOR LARGE-SCALE TRANSCRITICAL CO₂ HEAT PUMPS

Caio Coutto^(b), Armin Hafner^(a), Azam Thatte^(c), George Kleynhans^(d)

^(a) Norwegian University of Science and Technology, 7491 Trondheim, Norway, armin.hafner@ntnu.no

^(b) Ecole Polytechnique Fédérale de Lausanne, Lausanne, 1008, Switzerland

^(c) Energy Recovery, 1717 Doolittle Drive, San Leandro, CA, 94577, USA

^(d) MAN Energy Solutions Schweiz AG, Hardstrasse 319, 8005 Zürich, Switzerland

ABSTRACT

Transcritical CO₂ heat pumps are a promising renewable solution to provide medium and high temperature heat, such as for the supply of district heating networks (DHN). High expansion and compression energy losses are associated with such systems due to the combined effect of large temperature lift and CO₂'s high operating pressures. To reduce these losses and improve the system efficiency, several technologies that recover the expansion work, mainly turbines and ejectors, have been applied to replace throttling valves. Multi-phase rotary pressure exchangers (PXG) which are often used in seawater reverse-osmosis desalination plants have started to penetrate the refrigeration market but have not been tested yet for large-scale CO₂ heat pump applications. This study proposes to assess the potential of integrating PXG to large-scale transcritical CO₂ heat pump systems and to compare its increased efficiency with that of other technologies. Several new heat pump system architectures integrating the PXG were created and analysed in typical conditions for a very large capacity water-to-water heat pump with a turbo-compressor. The analyses show that PXG offers significant performance improvement, up to 10% COP increase, that is larger than that of existing state-of-the-art expanders which makes it a relevant option to consider in future systems.

Keywords: Heat Pumps, Transcritical, Carbon Dioxide, Turbo compressors, Rotary Pressure Exchanger, Energy Efficiency

1. INTRODUCTION

Heating and cooling applications in buildings and industry account for nearly half of the global total energy consumption and contribute to 38% of CO₂ emissions (IEA, 2024). Currently, only 13% of heat comes from renewable energy, in this context, industrial heat pumps are identified as a key solution to decarbonize medium and high temperature heat supply, for heat distribution systems currently using fossil fuels as the main energy source.

Following the Kigali Amendment to the Montreal Protocol, natural working fluids are expected to increasingly replace hydrofluorocarbon-based refrigerants in the next decades. In view of the so-called fourth generation refrigerants, CO₂ (R744) has emerged as a promising alternative working fluid, due to its multiple advantages: low GWP, zero ODP, wide availability and safety. Moreover, R744 transcritical systems have gained a lot of attention, since they were first proposed by Lorentzen and Pettersen (1993) and since then continuous research and development is performed to further improve the system performance, energy efficiency, and application areas.

Transcritical heat pumps operate across the refrigerant critical point and differ from usual heat pumps with respect to the process of heat rejection: instead of a condenser, a gas cooler rejects heat in the supercritical region with a temperature glide. Such systems can take advantage of CO₂'s favourable thermodynamic properties in its supercritical state, such as high volumetric heat capacity and density. At normal discharge pressures, transcritical R744 units achieve high temperatures and enables this technology to heat water to temperature levels of up to 90 °C, Wolscht et al. (2023). This means a suitable technology for existing- or new generation of DHNs.

At elevated return water temperature levels, and corresponding high discharge pressures, the expansion process through a simple high pressure control valve generates more flash gas and is, therefore, less efficient. Yang et al. (2005) found the high-pressure expansion valve (HPV) to be the component responsible for the largest exergy

losses. Therefore, considerable research has been conducted to find novel methods to improve the performance and energy efficiency of transcritical systems to be more competitive and render high temperature heat pump applications.

The recovery methods of expansion work were recognized as one of the main challenges, Song et al. (2022) and Yu et al. (2019), in recent development to improve the efficiency of transcritical cycles. The recuperated energy from the expansion can be used to reduce the compressor work through work recovery devices (WRD). The most common being ejector and turbine/expander technology, which both demonstrate advantages. However, ejectors are simple devices able to provide a limited pressure lift of about 10-15 bar, at maximum. Turbines or expanders, which are more efficient, suffer from high upfront and maintenance costs and generally limited to operate outside the vapour-liquid equilibrium region.

Zhang et al. (2013) has reviewed the potential of different types of two-phase turbines for transcritical systems in refrigeration, but none are yet in commercial operation. Little to almost no research in this field considers rotary pressure exchanger technology, also known as wave rotor, which is widely used in reverse osmosis desalination plants, despite its benefits being very recently demonstrated in refrigeration, for supermarkets, Sengupta and Dasgupta (2023).

A novel type of rotary pressure exchanger (PXG), shown in Fig. 1, adapted to multi-phase CO₂ operation has recently been introduced, Thatte (2022, 2023). It is a combined compression-expansion device able to directly transfer the expansion energy from a high-pressure flow to compress a flow at lower pressure, through direct fluid-to-fluid pressure exchange, with a high expansion work recovery ratio. Therefore, the integration of the PXG to recover expansion work is of particular interest but has not been implemented yet for large-scale heat pump systems. This study analyses the potential of this technology for transcritical R744 heat pump systems for very large DHNs by comparing its performance to other WRDs.

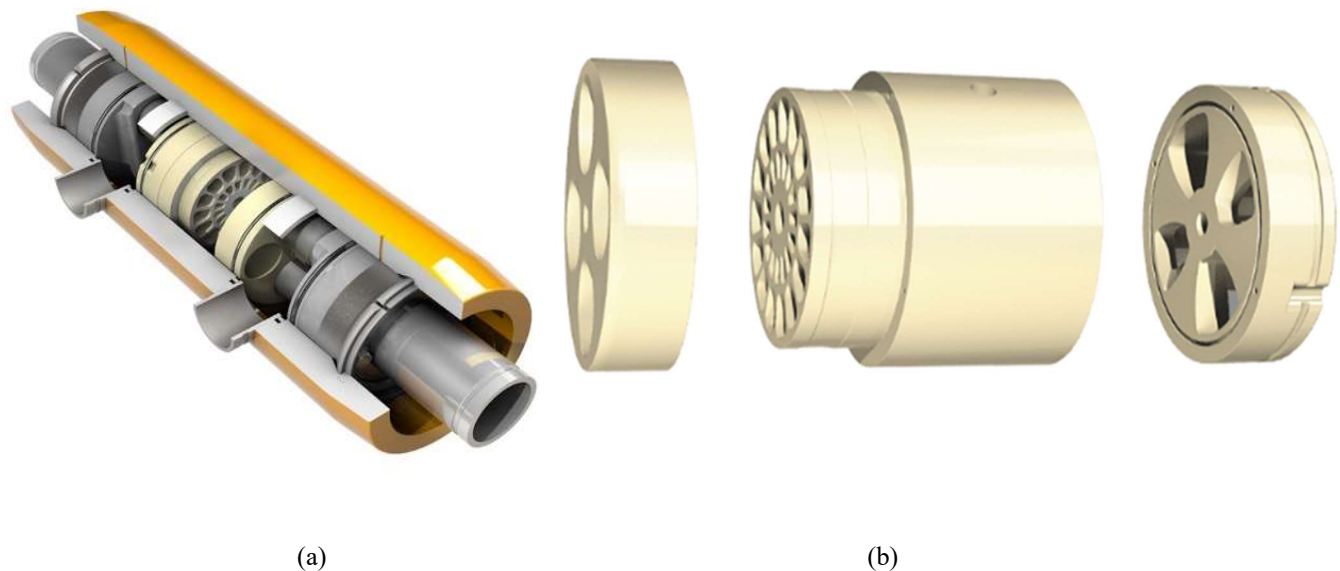


Figure 1: Rotary Pressure Exchanger: (a) cut-away view of PXG with the rotor at its centre, and (b) exploded view of the device

A set of transcritical heat pump cycle configurations, with specific large-scale constraints, such as integrated motor cooling (MC), featuring the PXG, alternative devices, and a baseline system without any WRD are proposed. These configurations are then analysed based on a reference case from a very large capacity existing DHN that uses seawater as a heat source. The proposed configurations are simulated with a static thermodynamic model that was developed using reliable industrial references for all the technologies evaluated.

2. SYSTEM ARCHITECTURES

2.1. System Description

Based on previous work, and on the large-scale application conditions, several new cycle configurations are proposed. The original R744 transcritical system, introduced by Lorentzen and Pettersen (1993) constitutes the baseline configuration designated as **a2**), is shown in Fig. 2 and provides comparison to different loops including PXG and/or turbines. This design includes the high-pressure control valve that adjusts the gas cooler (GC) pressure and refrigerant expansion to the evaporator pressure level. An internal heat exchanger transfers heat from the high side flow, downstream of the gascooler, to superheat the low-pressure side flow prior to compressor suction. In this way, the evaporator does not need to provide any superheat and can be maintained in flooded conditions, due to the receiver downstream and the exit of a certain amount of refrigerant towards the internal heat exchanger. The advantages of this configuration are two-fold: it enhances the evaporator heat transfer coefficient and enables maximum evaporator pressure, which in turn decreases the compressor pressure ratio. This is especially important for R744 systems because 1 K temperature difference represents 1 bar in pressure difference in this operational region.

In this large-scale application analysis, a multi-stage radial turbo-compressor is considered. MAN Energy Solutions' (MAN-ES) integrated and hermetic active magnetic bearing (AMB) equipped HOFIM motor-compressor is taken as a reference. The integrated high-speed motor and AMBs require cooling and, to avoid using an external cooling system, R744 in vapour phase from the cycle is sourced (as shown in the green loop) as cooling gas to control the temperature level of the electrical motor, and the heated cooling gas is returned to compressor suction to provide additional superheat.

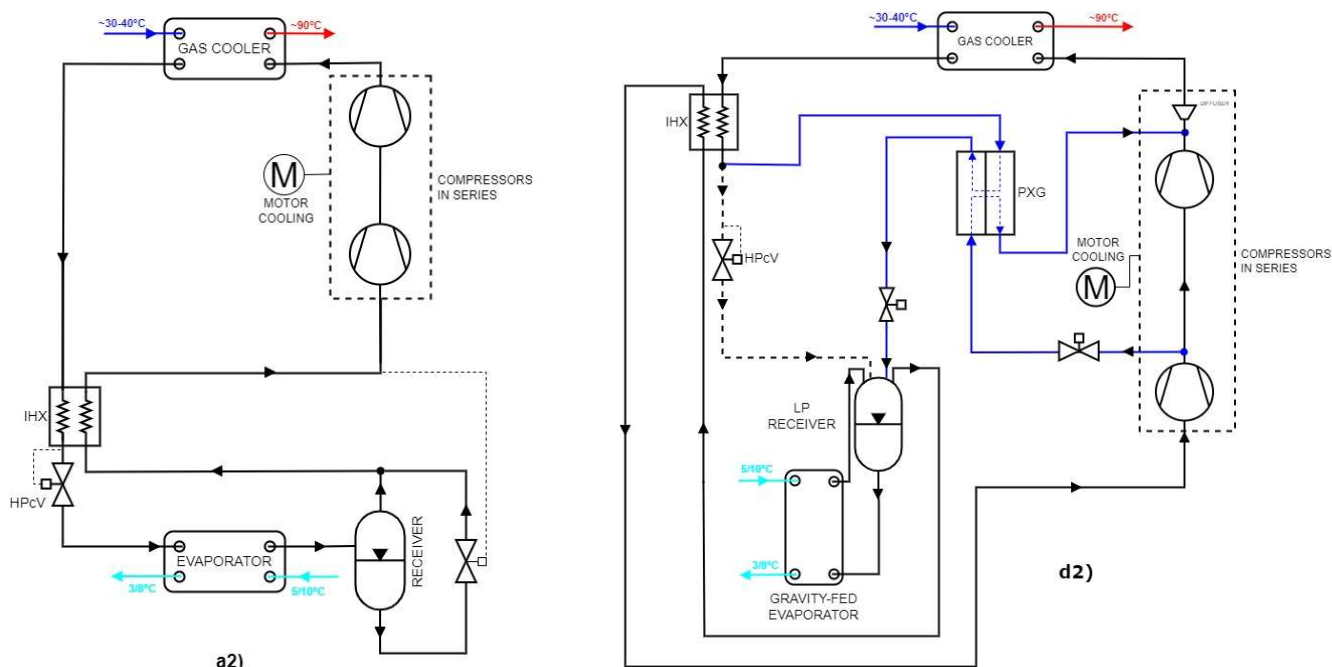


Figure 2: Baseline system **a2**) and PXG loop **d2**)

Despite having an excellent expansion work recovery ratio, i.e. pressure exchange efficiency, the PXG still has some pressure losses (ΔP_{PX}). About 2 bar is required, according to Thatte (2022), to achieve similar GC and evaporator pressures. To enable the PXG to function properly, a certain pressure difference is required, between the flows entering and exiting from opposite ends, Fig. 2 clarifies this aspect.

Figure 3 shows that if the PXG is applied to expand the flow from the system's maximum pressure (GC pressure)

to the system's minimum pressure (evaporator pressure); then, before entering the device, the LPin pressure must be raised by ΔP_{PX} to overcome the pressure losses inside the device and thereby to push out the LPout flow. The same applies for the HPout pressure level, which after exiting the PXG, must also be elevated by ΔP_{PX} to reach the GC pressure. Thatte (2022) applied two additional pressure lift devices to provide the required pressure boost at the inlet and the outlet of the PXG compression flow path.

The proposed loop integrating the PXG, hereafter referred to as *d2*), in Fig. 2, considers special connection ports to the multi-stage turbo-compressor and eliminates auxiliary pressure rise device requirement. The first compression stage can be used to provide the desired pressure lift for the PXG LPin flow. For the HPout flow, injection downstream of the final compression stage before entering the discharge diffuser is proposed. This novel concept avoids injecting it into the suction of the final compression stage, which would require another separate compression stage operating at a small pressure ratio, thereby increasing the pressure ratio on the other stages. In this way, PXG's LPin flow comes from the outlet of the first compression stage and HPout flow re-joins the main flow at the inlet of the final compressor diffuser.

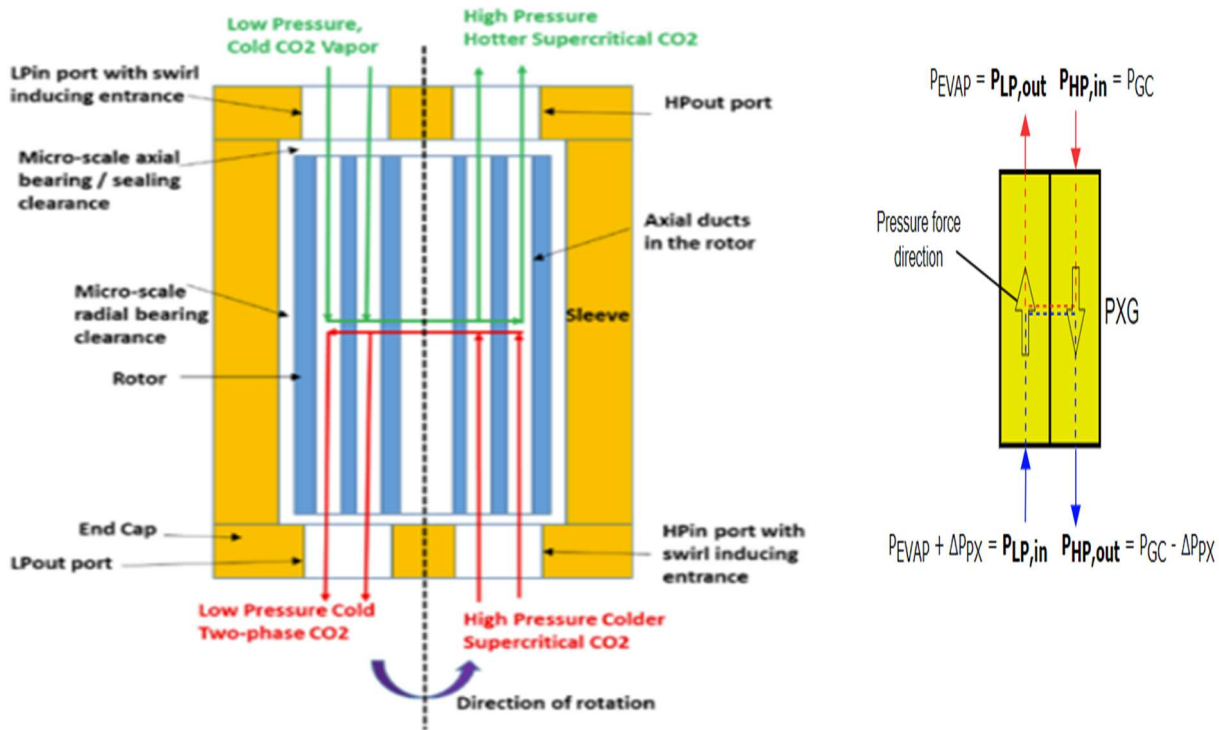


Figure 3: Schematic of the internal geometrical features of PXG and its flows

Various configurations, including turbines are developed to investigate the PXG performance versus the, theoretically, most efficient WRD alternative. Fig. 4 shows a configuration designed for a basic non-expanding turbine, referred to as f2A turbine that expands into the two-phase region, referred to as f4), which has not been industrially developed yet, can be a future competitor of the PXG. Both configurations, shown in Fig. 5, are similar to the baseline system a2), however, in f4), the two-phase turbine replaces the HPV and in f2), the basic turbine is located upstream the HPV, which keeps the turbine outlet outside the two-phase region while the valve performs the two-phase expansion. The f4) loop, utilizing all available expansion work, will yield higher energy efficiency values than f2). However, the interesting comparison is with the PXG loops, to investigate the potential performance differences.

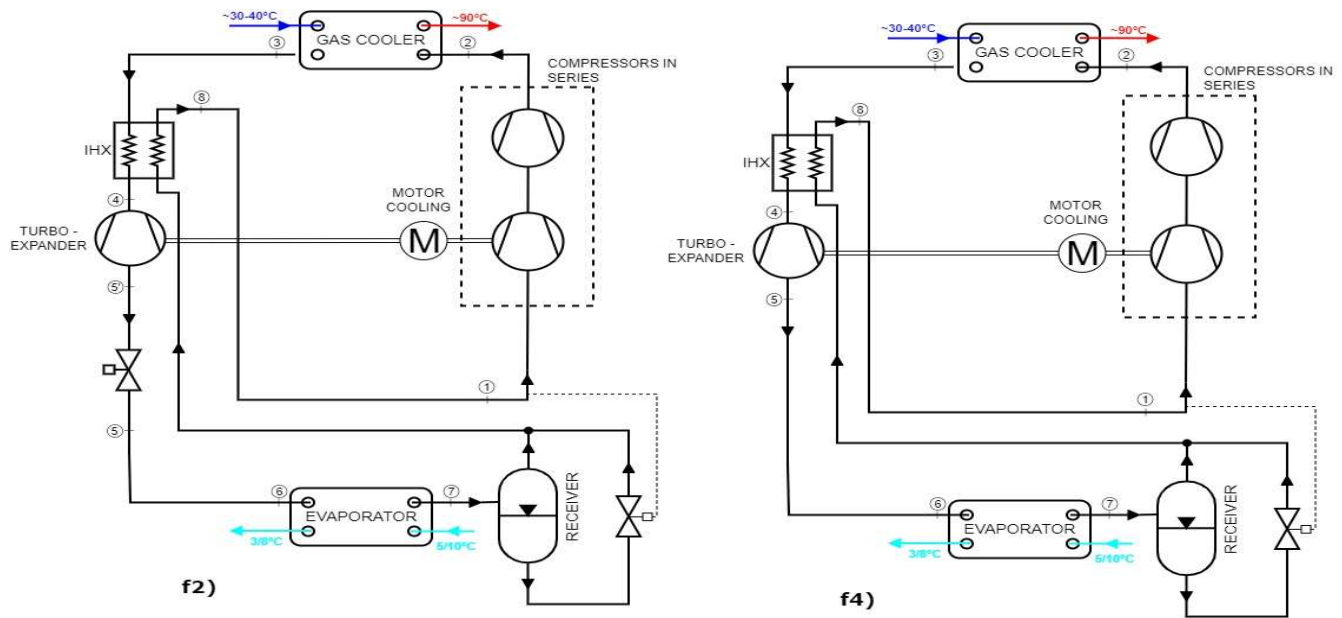


Figure 4: Turbine loops *f2)*: basic and *f4)*: two-phase

2.2. Methodology

When modelling transcritical systems, the GC pressure is an independent variable that adds a further dimension to the problem. Previous works on R744 transcritical systems highlighted that there exists a theoretical optimum for the discharge pressure which maximizes the COP, Neksa (2002). In this case, the model guesses the discharge, or high side, pressure level from a range of values in the supercritical region from 95 to 135 bar and solves the system for each of them. Then, the discharge pressure corresponding to the maximum COP is retained. Note that the final optimal value may still change, after verifying the consistency of the found pressure value, with the assumed pinch point of the GC – more details are provided in the description of the GC model.

The solving method consists of applying energy and mass balances to every single component. Because there are several internal loops in the system, the system cannot be solved in an implicit manner and an iterative procedure is required to calculate the correct flow rates and enthalpies. A *Matlab* code is written to solve the equations and upon convergence for mass (flow rates) and energy (enthalpies), the thermodynamic properties are calculated at all state points with the *REFPROP* fluid property database.

The reference boundary conditions are for an example large DHN in a Nordic environment with seawater heat source. A heat duty of $Q_{sink} = 15 \text{ MW}$ at the corresponding supply- and return water temperatures $t_{in} = 40^\circ\text{C}$ and $t_{out} = 90^\circ\text{C}$ are considered. The most representative condition is defined for a seawater temperature level of $t_{sw,in} = 5^\circ\text{C}$. The maximum allowed seawater temperature difference across the secondary fluid side of the evaporator is $\Delta t_{sw} = 2\text{K}$.

Two parameters are varied to generate more cases representing a wider range of operating conditions: the DHN water return temperature and the seawater source temperature. The DHN return temperature t_{in} set comprises five values centered around the reference level to account for the differences between older and more recent DHNs. Similarly, the seawater temperature $t_{sw,in}$ set contains 4 values representing the temperature transition between seasons.

$$t_{in} = \{30; 35; 40; 45; 50\}^\circ\text{C}$$

$$t_{sw,in} = \{2; 5; 10; 15\}^\circ\text{C}$$

For the PXG, a 1D thermodynamic model based on Thatte (2023) is used and assumes mass conservation because the leakage losses are negligible. The maximum flow rate from LPin is governed by the mass boost ratio (MBR), in Eq. (1), and usually it is attained. The device is also considered to be adiabatic, i.e., all the energy generated from the expansion process is transferred to the compression process; hence, no loss term in the energy balance in Eq. (2) and Eq. (3). The energy balance couples the expansion and compression efficiencies with one of them assumed (here the expansion efficiency) and the other is calculated in Eq. (4).

$$\dot{m}_{LP,in,max} = MBR \cdot \dot{m}_{HP,in} \quad \text{Eq. (1)}$$

$$h_{LP,out} = h_{HP,in} + \frac{h_{LP,out,s} - h_{HP,in}}{\eta_{PX,comp}} \quad \text{Eq. (2)}$$

$$h_{HP,out} = h_{LP,in} + \frac{\dot{m}_{HP,in}}{\dot{m}_{LP,in}} \cdot (h_{HP,in} - h_{LP,out}) \quad \text{Eq. (3)}$$

$$\eta_{PX,comp} = \frac{h_{HP,out,s} - h_{HP,in}}{h_{HP,out} - h_{LP,in}} \quad \text{Eq. (4)}$$

3. RESULTS

This chapter presents the results of the simulations and the various analyses performed for the defined set of configurations described above. The results are obtained through an optimization procedure to find the highest COP, with a GC pinch point constraint, after solving the energy- and mass balances. This section presents a comprehensive tabular comparison of the results, for all investigated configurations, using the most representative reference boundary conditions, defined in the methodology. The results for the less typical operational conditions are also presented in graphical form with standard condition variation.

The COP increase with respect to the baseline **a2)** of the different configurations are reported in Table 1, as well as the corresponding Carnot efficiency. The corresponding GC pressure, inlet pressure of the second compression stage $P_{comp,2}$ and mass flow rates of different components are presented in Table 2.

Table1. Efficiencies of the various configurations

Circuit	a2)	d2)	f2)	f4)
$\Delta COP / COP$	-	10%	6%	10%
η_{Carnot}	53.1%	58.3%	56.5%	58.3%

Table2. Pressure and Mass Flow Rates

Circuits	a2)	d2)	f2)	f4)
$P_{GC} [bar]$	113	113	113	113
$P_{comp,2} [bar]$	arbitrary	39.1	arbitrary	arbitrary
$\dot{m}_{ref} \left[\frac{kg}{s} \right]$	57.3	57.2	57.34	57.46
$\dot{m}_{LP,in} \left[\frac{kg}{s} \right]$	-	5.29	-	-

The two main expansion devices (PXG and turbines) were assumed to operate at the same isentropic efficiency of

80 %. For the basic turbine, which is the current state of the art solution, measurement results exist to support this assumption. However, for the PXG and two-phase turbine, which do not yet have industrial references in transcritical CO₂ heat pump applications, it is more robust to compare the PXG vs. two-phase turbine performances over a range of possible efficiency values. The 80 % hypothesis was the considered as the efficiency target to meet the performance of existing basic turbine, hence the expansion efficiency was reduced in the sensitivity analysis.

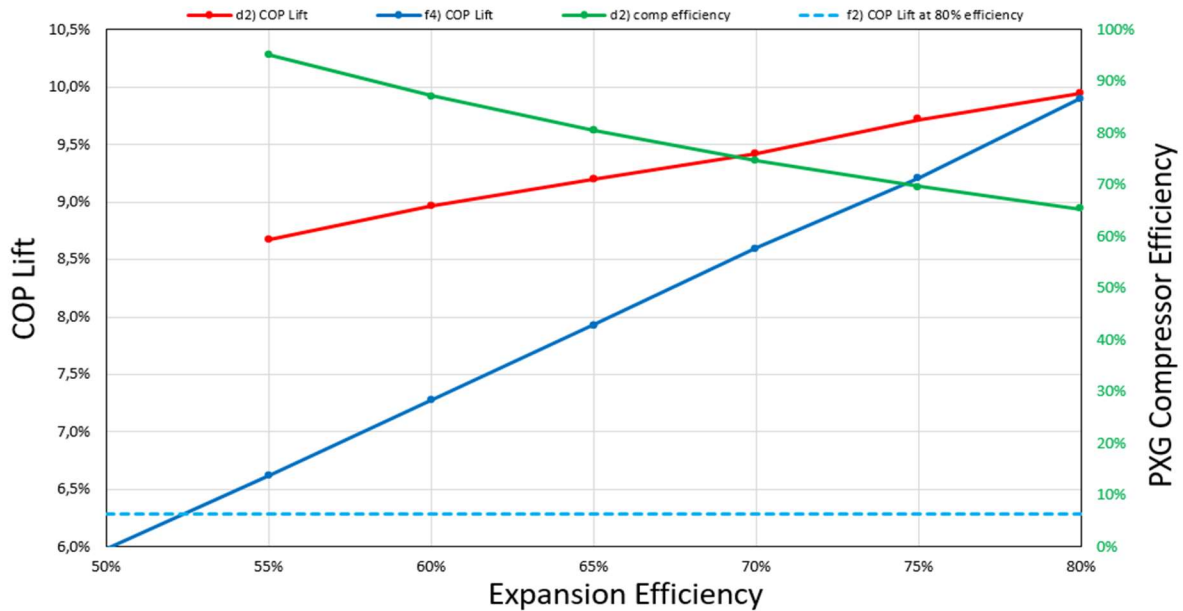


Figure 5: Variation of COP with Expansion Efficiency for the *d2)* and *f2)* configuration

In Fig. 5, the COP values were recalculated for the PXG loop *d2)* and the same was done for *f4)*, by varying the expansion efficiency from 80 % down to 50 % with 5 % incremental steps. Below 50-55 % expansion efficiency, the PXG cannot operate, otherwise the compression efficiency, which is coupled, would exceed 100 %. Therefore, the corresponding compression efficiency (red curve) is also plotted on the secondary axis, on the right hand side. Finally, the COP reference value of the basic turbine is also shown, in the black dotted line.

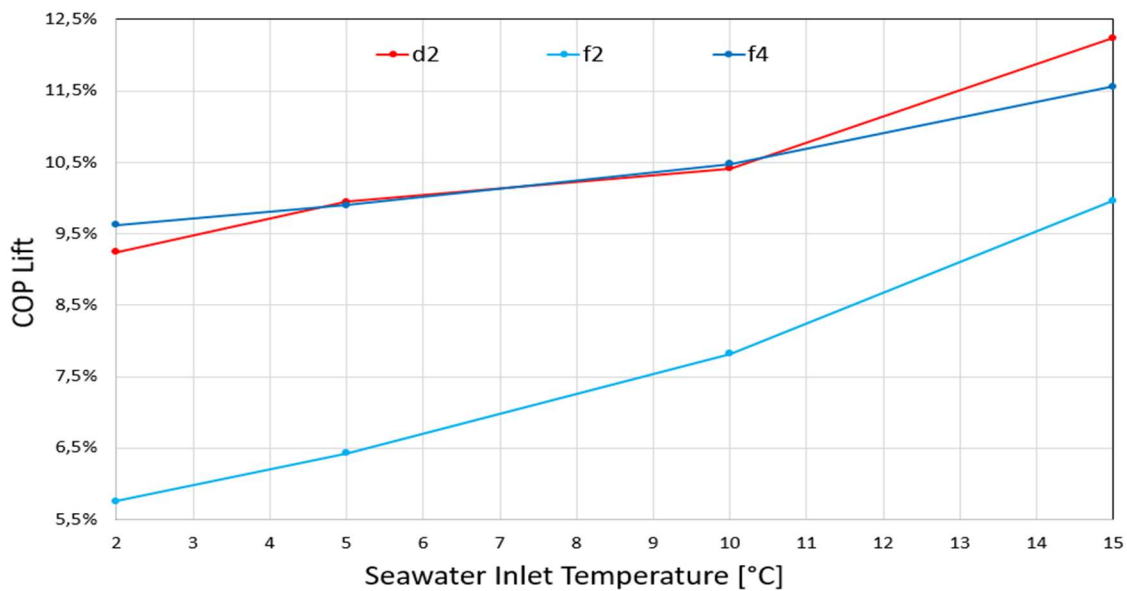


Figure 6: COP lift as function of the seawater inlet temperature

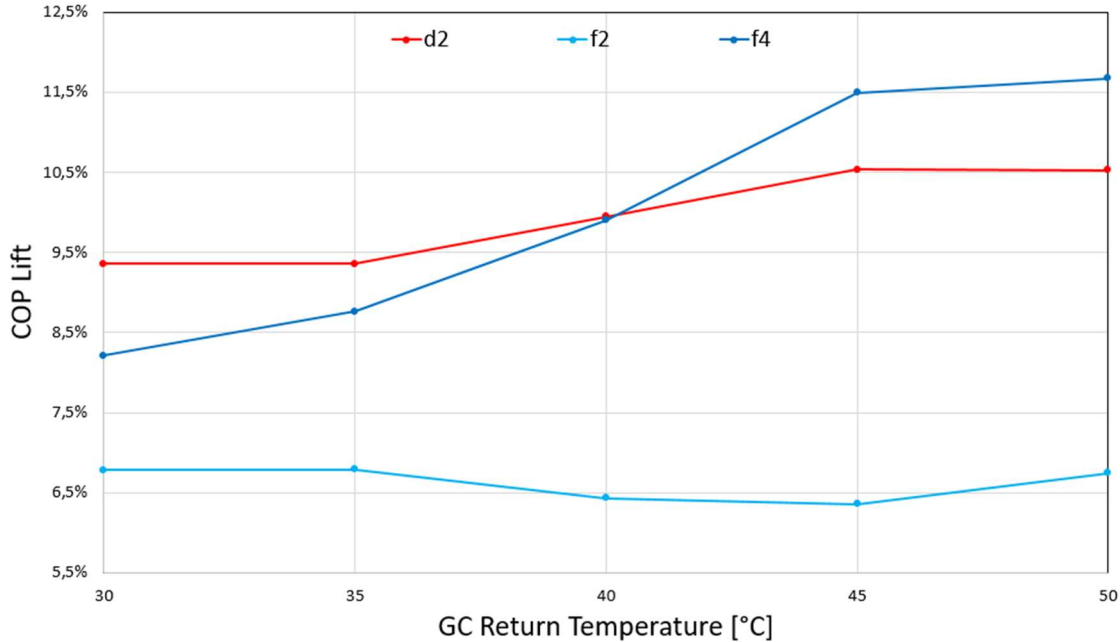


Figure 7: COP lift as function of the gascooler return temperature

The COP are recalculated and plotted for a set of different boundary conditions that were defined in the methodology. The effect of DHN return temperature and seawater source temperature changes are treated separately and shown in Fig. 6 and Fig. 7, respectively. The COP improvement with respect with the baseline loop *a2*) COP (showed in the histograms) is plotted for all the other configurations.

4. DISCUSSION

Comparing the the PXG *d2*) with the basic turbine *f2*), the latter is considerably less efficient in all operating conditions because the turbine cannot operate over the full system pressure range like the PXG. In addition, the potential two-phase turbine is limited by the saturation pressure, at around 57 bar, in the reference case. This determines that a third of the pressure ratio is not available and thus, not as much compressor work can be recovered. Furthermore, this also increases the MC requirement, compared to *d2*) or *f4*) which recover more work, and requires more MC flow to be extracted before the turbine.

Only at a high seawater temperature, above 15°C, the basic turbine reduces the gap with the other configurations. This can be explained as the suction pressure is increased, so the share of expansion work available in the two-phase region is reduced. Otherwise, its COP increase is at least 2 – 3 % lower than *d2*) and *f4*) configurations, which are the best performing systems.

The break-even in COP increase, between basic and two-phase turbines, appears only below 55 % of expansion efficiency for the two-phase device, versus an 80% efficient basic turbine. Furthermore, in the feasible operational range of the PXG, there is no break-even between the two technologies and the COP increase of *d2*) is at minimum 2% higher than *f2*). In terms of cost, it is expected to be more expensive compared to the PXG solution, which does not require much additional components, and is also similar in terms of piping pressure losses. This however doesn't consider auxiliary system that may be needed to start-up or shut down large scale heat pump system or still unknown effect of the integrated PXG solution when considering off-design and transient operation. This could be further investigated in a future study.

When comparing the PXG solution *d2*) with the two-phase turbine *f4*), both configurations achieve the highest COP increases, with a 10 % lift with respect to the baseline *a2*) because both systems work very similarly: they have roughly the same expansion work available and despite reusing it in different ways, the energy is kept within

the system. They both operate at a pressure of around 113 bar and a mass flow rate of around 57 kg/s. This difference between both systems are more notable in the results, when looking at the sensitivity analysis.

Fig. 5 shows that as the expansion efficiency is reduced, the COP of *d2*) is more advantageous than *f4*). A lower expansion efficiency, in *f4*), means that the turbine can recover less compressor work, which increases MC flow and leads to a further decrease in the mass flow to the turbine and so forth. This is not the case with *d2*) because the efficiency of the system is less dependent on the MC flow, as the MC does not compete with the PXG for flow rate, but rather works together. In this way, the COP of *d2*) is less affected by a lower expansion efficiency of PXG and is still provides a higher COP lift than the basic turbine by a margin of 2%.

It is worthwhile to note that the system with PXG at 55% expansion efficiency has the same COP as the two-phase turbine at 75% efficiency. Even in the more optimistic projections for two-phase turbines to reach the same efficiency as single-phase devices, the PXG can still perform equally, if not better, with a poorer expansion efficiency, in this particular configuration with significant MC load. Because there are no references for the efficiency of both devices, when used in large-scale transcritical R744 heat pumps, these results reduce the uncertainty and show that the PXG's potential is more robust than the two-phase turbo-expander.

When the boundary conditions are varied towards more favourable operational conditions, i.e. lower DHN return water temperatures or higher seawater supply temperature (see Fig. 6), yielding higher COPs for all systems, the advantage of *d2*) over *f4*) is reduced. On the contrary, when the DHN return water temperature is increased, the optimal GC pressure of *f4*) increases more than that of *d2*), and determines that more expansion work can be recuperated and consequently, be more efficient. However, this boundary condition adversely affects the efficiencies of all systems and modern DHNs try to avoid high water return temperatures for other reasons, such as heat losses. Therefore, it is not really that problematic for a PXG configuration if the DHNs return water flow rates are 30-35°C. In this case, the PXG configuration would provide a COP lift of 9%, which is at least 1% higher than the other configurations including *f4*).

When looking at the complexity of the systems on a purely steady-state design analysis, *d2*) shows to be a good compromise between and system cost. *f4*) would be more costly and could be challenging to control, especially because of the flashing downstream of the turbine. In summary, the *d2*) loop which features the PXG, has the potential to increase the efficiency of large-scale R744 transcritical heat pumps by around 10% in most operation conditions. In most cases, especially in the more likely conditions, the PXG performs as well as or better than the two-phase turbine alternative.

5. CONCLUSION

This study indicates that the PXG can be more competitive than the two-phase turbine device, which is still in development, for at least three reasons. Firstly, the PXG can provide a COP increase of about 10% at nominal operating conditions, which is twice as much as with existing turbines and only matched by the system with an ideal two-phase turbine. On top of that, its enhancement of the system performance is more robust when varying the isentropic efficiency of both devices to less optimistic values; the COP increase with the PXG is the largest and stays in the range of 9-10.5%, even when assuming lower efficiencies. Secondly, when considering lower DHN return water temperatures, below 40 °C, such as in more recent generations of DHNs, the PXG can provide higher COP increases (around 9%) than the turbine, which is less efficient in this domain. Thirdly, the best performing PXG configuration is the one with the simplest design: with minimal additional devices, such as valves or ejectors, and thus would neither significantly increase the control complexity of the heat pump, nor the cost compared to highly engineered theoretical two-phase turbines.

Finally, the investigations shows that the PXG configuration has the potential to improve the efficiency of large-scale R744 transcritical heat pumps by a significant value when compared to devices currently in use. It is at least as competitive as the best performing WRD that can be developed in the future. This stimulates more interest in continuing to investigate the development and use of R744 heat pumps with PXG, with experimental validation, for new applications. These results are encouraging to initiate new development steps to push the limits of industrial heat pumps to further decarbonize more sectors.

ACKNOWLEDGEMENTS

The authors gratefully acknowledge the Research Council of Norway for the financial support for carrying out the present research [NFR Project No. 308847 PCM-STORE].

NOMENCLATURE

<i>PX,LP</i>	PXG Low pressure port	<i>MBR</i>	Mass Boost Ratio
<i>PX,HP</i>	PXG High pressure port	<i>PXG</i>	CO ₂ multi-phase Pressure Exchanger
<i>out</i>	Outlet	<i>DHN</i>	District Heating Network
<i>in</i>	Inlet	<i>WRD</i>	Work Recovery Device
<i>sw</i>	Seawater	<i>COP</i>	Coefficient of performance
<i>MC</i>	Motor cooling	<i>HPV</i>	High Pressure Valve
<i>ref</i>	Refrigerant	<i>GC</i>	Gas Cooler
<i>comp</i>	Compressor	<i>h</i>	Enthalpy (kJ/kg)
<i>s</i>	Isentropic	<i>m</i>	Mass flow (kg/s)
<i>exp</i>	Expansion	η	Isentropic efficiency

REFERENCES

- Wolscht, L., Kleyhans, G., Somaini, R., Baumann, U., TPS Conference 2023 (Houston, TX). Full scale testing of a 36 MW CO₂ heat pump in two-phase flow condition.
- Ye, Z., Wang, Y., Song, Y., Yin, X., Cao, F., 2020. Optimal discharge pressure in transcritical CO₂ heat pump water heater with internal heat exchanger based on pinch point analysis. *Int. J. of Refrigeration*, 118:12–20.
- Lorentzen, G., Pettersen, J., 1993. A new, efficient and environmentally benign system for car air-conditioning. *Int. J. of Refrigeration*, 16(1):4–12.
- Yang, J.L., Ma, Y. T., Li, M.X., Guan, H.Q., 2005. Exergy analysis of transcritical carbon dioxide refrigeration cycle with an expander. *Energy*, 30(7):1162– 1175.
- Yu, B., Yang, J., Wang, D., Shi, J., Chen, J., 2019. An updated review of recent advances on modified technologies in transcritical co₂ refrigeration cycle. *Energy*, 189:116147.
- Zhang, Z., Ma, Y., Li, M., Zhao, L., 2013. Recent advances of energy recovery expanders in the transcritical CO₂ refrigeration cycle. *HVACR Research*.
- Sengupta, A., Dasgupta, M.S., 2023. CFD supported thermodynamic analysis of a CO₂ pressure exchanger based refrigeration system for supermarkets. *Int. J. of Refrigeration*, 152:110–121.
- Thatte A., et. al., 2022, Novel Rotary Pressure Exchanger for Highly Efficient Trans-Critical CO₂ Refrigeration Cycle, *Proceedings of International Institute of Refrigeration (IIR), Gustav Lorentzen Conference on Natural Refrigerants, Trondheim, Norway, 56, 2022.*
- Thatte A., et. al., 2022, New Types of Low Global Warming, Energy Efficient Refrigeration Architectures Using a Trans-Critical Rotary Pressure Exchanger”, *Proceedings of ASHRAE, Toronto, Canada.*
- Thatte, A., 2023. Multi-Phase Rotary Pressure Exchanger as a Novel Compressor-Expander for Increasing Efficiency of Trans-Critical CO₂ Heat Pumps, *Proceedings of ASME Turbo Expo 2023, GT2023-104173, V012T28A031; 13 pages.*
- Nekså, P., 2002. CO₂ heat pump systems. *Int. J. of Refrigeration*, 25(4):421–427.